Future Temperature Related Deaths in the U.S.:

The Impact of Climate Change, Demographics, and Adaptation

Jangho Lee and Andrew E. Dessler

Department of Atmospheric Sciences, Texas A&M University, College Station, TX, USA

Correspondence: Jangho Lee (jangho.lee.92@tamu.edu)

Abstract

Mortality due to extreme temperatures is one of the most important impacts of climate change. In this analysis, we use historic mortality and temperature data from 106 cities in the United States to develop a model that predicts deaths attributable to temperature. With this model and projections of future temperature from climate models, we estimate temperature-related deaths in the United States due to climate change, changing demographics, and adaptation. We find that temperature-related deaths increase rapidly as the climate warms, but this is mainly due to an expanding and aging population. For global average warming below 3°C above pre-industrial levels, we find that climate change slightly reduces temperature-related mortality in the U.S. because the reduction of cold-related mortality exceeds the increase in heat-related deaths. Above 3°C warming, whether the increase in heat-related deaths exceeds the decrease in cold-related deaths depends on the level of adaptation, emphasizing the need for our society to effectively adapt to climate change that we do not avoid. Most of the reduction in mortality is occurring in the Southern U.S. This region is already well adapted to hot temperatures and the reduction of cold-related mortality drives overall lower mortality. Cities in the Northern U.S. are not well adapted to high temperatures, so the increase in heat-related mortality exceeds the reduction in cold-related mortality. Thus, while the total number of climate-related mortality may not change much, climate change will shift mortality to higher latitudes.

1. Introduction

The relationship between temperature and human mortality has been the subject of many previous studies (Berko, 2014; Bobb et al., 2014; Demoury et al., 2022; Dimitrova et al., 2021; Gasparrini & Armstrong, 2011; Gasparrini, Guo, Hashizume, Lavigne, et al., 2015; Guo et al., 2011; Kalkstein & Greene, 1997; Ma et al., 2015; Yi & Chan, 2015; Zhang et al., 2016). Previous studies have projected future temperature-related mortality covering different regions, such as global major cities (Gasparrini et al., 2017; Takahashi et al., 2007; Vicedo-Cabrera et al., 2018), the U.S. (Knowlton et al., 2007; Petkova et al., 2017; Jackson et al., 2010; A. I. Barreca, 2012; Wang et al., 2016; Anderson et al., 2018; Lo et al., 2019; Weinberger et al., 2017), cities in Europe (Hajat et al., 2014; Martínez-Solanas et al., 2021; Muthers et al., 2010), or Asia (Lee & Kim, 2016; Yang et al., 2021). Using historical data sets, previous studies have found that temperature and mortality show a V-shaped curve, where mortality increases as temperatures become very hot or very cold (Dimitrova et al., 2021; Gosling et al., 2009; de Schrijver et al., 2022; Vardoulakis et al., 2014; Berko, 2014). Thus, we expect climate change to influence temperature-related mortality.

Another issue we explore in this paper is the impact of demographics. Older populations are known to be more vulnerable to temperatures extremes (Bobb et al., 2014; Anderson et al., 2018; Åström et al., 2013; Barnett, 2007; Hintz et al., 2018; Lin et al., 2011; Lee & Kim, 2016; Yi & Chan, 2015; Zhang et al., 2016; de Schrijver et al., 2022), and since population is projected to both age and grow globally, the compound effect of demographic and population changes will increase temperature-related mortality (Li et al., 2016; Marsha et al., 2018). Previous studies included demographic and population change in their projection (Hajat et al., 2014; Deschênes & Greenstone, 2011; Deschenes & Moretti, 2009; Lee & Kim, 2016; Jenkins et al., 2014; Petkova et al., 2017; Vardoulakis et al., 2014; Li et al., 2016), mostly using population projections from shared socioeconomic pathways (SSPs) (Hauer, 2019).

It is also clear that people will take actions to head off the impacts of extreme temperatures (A. Barreca et al., 2016; Folkerts et al., 2020; Fouillet et al., 2008; Carson et al., 2006; Davis et al., 2003; Gasparrini, Guo, Hashizume, Kinney, et al., 2015; Kyselý & Plavcová, 2012). However, such adaptation takes resources, which many people do not have, so how well this can be done is an uncertainty that any analysis of future temperature-related mortality must address.

There are few ways to incorporate adaptation to the future projections. Previous studies simply shifted the temperature-mortality relationship to warmer temperatures (Jenkins et al., 2014; Folkerts et al., 2020; Gosling et al., 2009), extrapolated the historical trends of temperature-mortality relationship (Muthers et al., 2010; Petkova et al., 2017), or adjusted the slope of temperature-mortality relationship (Jenkins et al., 2014). Here we use an “analog city” approach (Heutel et al., 2021; Knowlton et al., 2007; Kalkstein & Greene, 1997), where the mortality model for a city with warmer climate is applied to cooler city in a warming climate. For example, in Knowlton et al. (2007), they assumed that New York in the 2050s will have similar temperature-mortality relationship as Washington and Atlanta in 1973-1994, since temperatures in New York in 2050s are similar to temperatures in Washington and Atlanta in 1973-1994.

In this paper, we consider all three of the factors that will impact future temperature-related mortality: climate change, population and demographics change, and adaptation, in order to determine how important each factor is.

2. Temperature-Mortality Relationship

Mortality data from the National Morbidity Mortality Air Pollution Study (NMMAPS) (Samet et al., 2000) contain the number of daily non-accidental deaths, stratified by age group (<65, 65-75, >75). We aggregate the two younger age groups to create a single category for ages <75. Data are collected from 106 large U.S. cities (Fig. 1a), which contain 65% of the population in the US, and cover the period from 1987 to 2000. Population data are also included in NMMAPS, which come from the National Center for Health Statistics (NCHS).

Historical hourly 2-m air temperatures from ERA-5 Land reanalysis (Muñoz-Sabater et al., 2021) are averaged to obtain daily average temperatures. The data have a horizontal resolution of 0.1°×0.1° and the average of the 9 grid points nearest to the center of each city are used to represent the daily average temperature of the city.

Following the framework of Gasparrini, Guo, Hashizume, Kinney, et al. (2015) and Gasparrini, Guo, Hashizume, Lavigne, et al. (2015), we use a Distributed Lag Non-Linear Model (DLNM) to describe the association between temperature and mortality. We model the daily number of deaths as a function of daily average temperature separately for each city and age group (under 75 and over 75). An important advantage of the DLNM is that it captures the lagged effect of temperature, where consecutive extreme days results in higher mortality than a single-day event (Gasparrini & Armstrong, 2011; Wang et al., 2016).

Previous studies reported that the impact of a hot day can extend for up to 3 days, while the impact of a cold day could extend 21 days (Demoury et al., 2022; Dimitrova et al., 2021). Therefore, we include lags of up to 21 days in the DLNM model. We also include the day of week to account for the weekly cycle, day of year for the annual cycle, and year for the long-term trend. A detailed explanation of the DLNM model used in this study can be found in section S1 of the supplement.

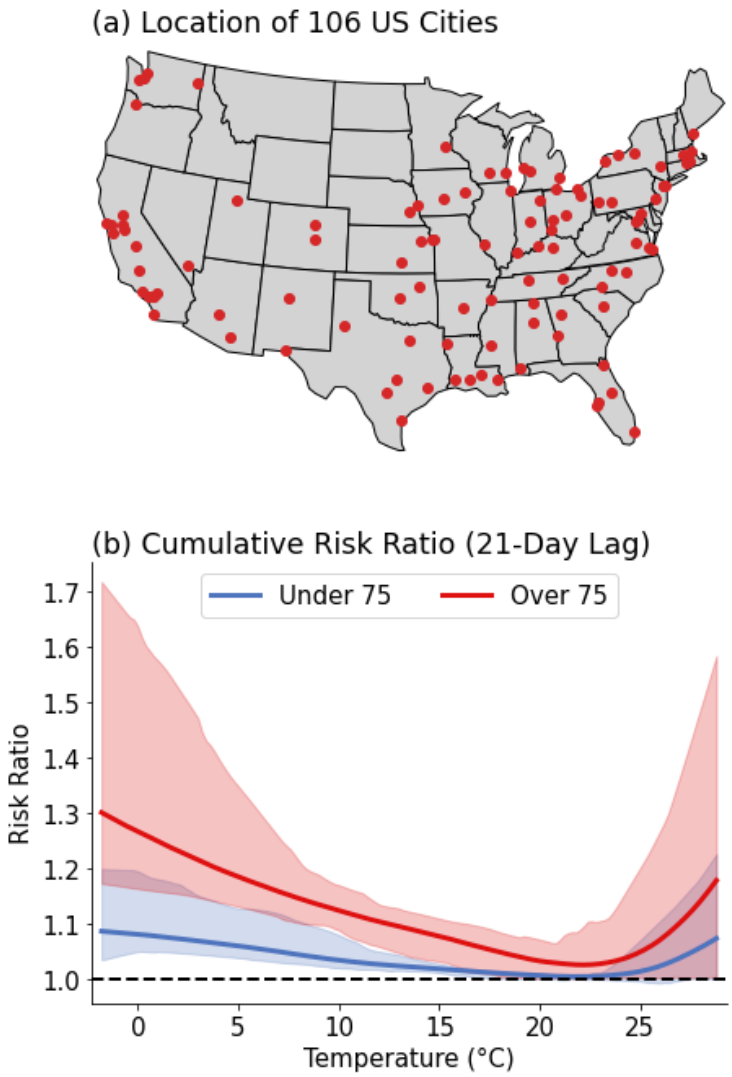

Figure 1. (a) Location of 106 cities used in this study. (b) Risk ratio (RR) of under/over 75 age groups, averaged for all cities in this study. Shaded regions show the 5th percentile to 95th percentile range of RR curve for all cities. RR is the number of deaths at each temperature divided by the number of deaths at the curve's minimum (the MMT), around 22°C.

3. Historical Temperature-Related Mortality

Fig. 1b summarizes the mortality risk as a function of temperature, averaged over all cities (curves for 25 most populated individual cities can be found in Fig. S1). The quantity plotted here, the cumulative relative risk (RR), is the number of deaths at each temperature divided by the number of deaths at the minimum mortality temperature (MMT), after summing the RR at each lag, up to 21 days. Our curve is similar to those found in previous work (Gasparrini, Guo, Hashizume, Kinney, et al., 2015; Gasparrini, Guo, Hashizume, Lavigne, et al., 2015; Gasparrini et al., 2017; Guo et al., 2011; Lin et al., 2011; Zhang et al., 2016; Ma et al., 2015; Yi & Chan, 2015).

With the regression models for each city and age group, we calculate the number of temperature-related excess deaths in the NMMAPS data in two steps. First, we define baseline deaths, which is the number of deaths at the MMT, calculated by averaging the number of deaths at temperatures around MMT (±0.5°C). With this baseline death value, we then calculate the number of deaths in each city using observed temperatures and the mortality-temperature curves.

There are an average of 36,444 temperature-related deaths per year between 1987-2000 (solid line in Fig. 2a). There is a clear trend over this period, and we can remove the effect of population changes by dividing the number of excess deaths by the population in each year, and then multiplying by the average population over the period. Doing this removes most of the trend (dashed line in Fig. 2a).

We will separate temperature-related deaths occurring above and below MMT, which by convention we refer to as heat- and cold-related deaths. We estimate there are an average of 4,819 heat-related deaths per year and 31,625 cold-related deaths. This is consistent with previous work that also found that most of the deaths were due to cold, rather than heat (Vardoulakis et al., 2014). We also found that 75.3% of deaths are from older (over 75) age groups (1 standard deviation of inter-city variance = 6.2%). The older age group is responsible for 75.6% (1σ=4.6%) and 75.1% (1σ=6.9%) of the heat- and cold-related mortality, respectively, despite being only 5.1% (1σ=1.3%) of the population. This point will be important later in the paper.

While 86% of temperature-related deaths are cold-related mortality, most of the deaths categorized as “cold-related” occur at temperatures only slightly below the MMT, which is typically around 22°C. While the risk of temperature-related death for these pleasant temperatures is low, these temperatures occur so frequently that a significant number of deaths nevertheless is occurring at these temperatures, a point also made by Gasparrini, Guo, Hashizume, Lavigne, et al. (2015).

This motivated us to look at mortality caused by significant heat and cold. For each city, we select the 30 days with highest and lowest temperatures, which we refer to as significant heat- and cold-related deaths (Fig. 2d and 2e). Summing up all cities, there are on average 2,607 deaths per year due to significant heat, and 6,894 due to significant cold, which are 54% and 21% of total heat and cold related deaths, respectively. Thus, heat-related deaths tend to be more skewed towards extreme heat while cold deaths are less so.

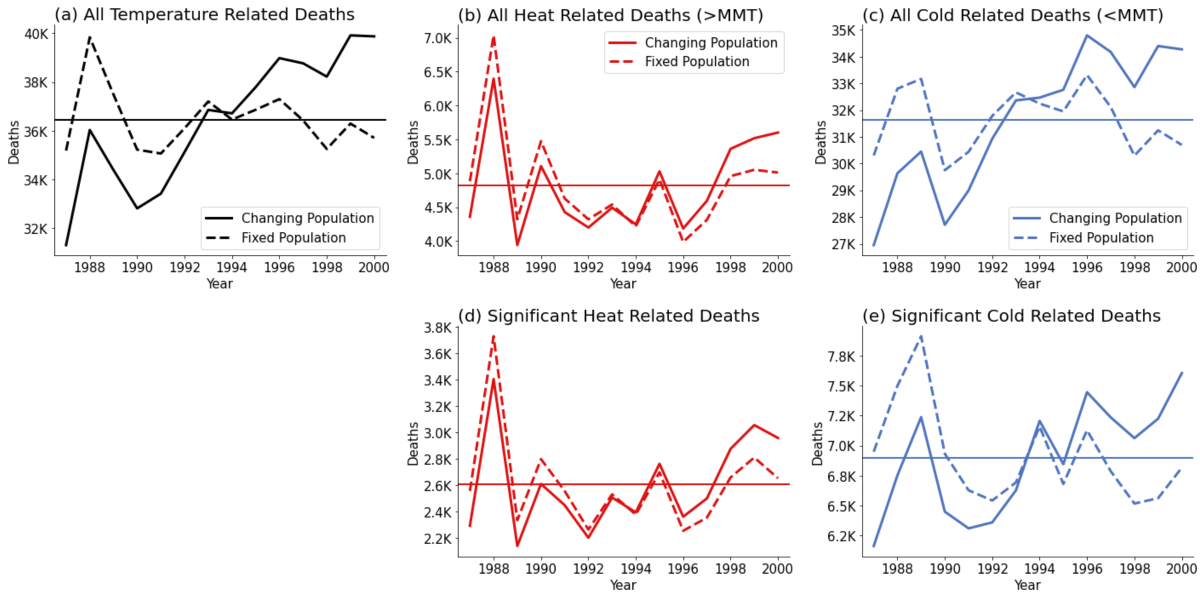

Figure 2. Time series of temperature-related deaths, summed over all 106 cities. (a) Solid line represents all temperature related deaths, while dashed line represents all temperature related deaths with fixed population (average population over 1987-2000 period). (b) Same as (a), but for heat-related deaths. (c) Same as (a), but for cold-related deaths. (d) Time series of deaths in the 30 days with highest temperatures. (e) Same as (d), but for lowest temperatures.

4. Measuring Adaptation

We quantify the effects of adaptation by comparing cities with different climates, an approach that has been used previously (Knowlton et al., 2007). In our implementation, for each city, we calculate the linear slope of cumulative RR versus temperature for temperatures above the MMT (hot RR slope) and slope of RR below the MMT (cold RR slope). While the RR curves are not linear, the linear fit is a metric for how steeply the curve rises. We do this fit separately for each age group. Fig. 3a and 3c show the hot RR slope regressed against median of daily average temperatures of the hot season (June, July, and August, JJA) of the 1987-2000 period. Fig. 3b and 3d show the cold RR slope regressed against the median daily average temperature of the cold season (December, January, and February, DJF).

There is a clear anti-correlation between the RR slopes and the cities' seasonal temperatures.

Cities with warmer summers are less vulnerable to heat-related mortality (hot RR slopes closer to zero, Fig. 3a, c), while cities with colder winters are less vulnerable to cold-related mortality (cold RR slopes closer to zero, Fig. 3b, d). One can think of these fit lines in Fig. 3 as measures of existing adaptation to hot and cold climates (Heutel et al., 2021; Knowlton et al., 2007; Gasparrini, Guo, Hashizume, Lavigne, et al., 2015; Kalkstein & Greene, 1997).

We do not know how people will adapt as the climate warms, so we analyze two limiting scenarios. The first is no further adaptation. For this, we assume the RR curve of each city remains fixed at values obtained from the 1987-2000 mortality data as climate warms (Fig. S1). Our second scenario, which we consider to be a strong adaptation case, assumes that, as each city warms up, the hot side of the city's mortality curve decreases following the slope of the regression lines in Figs. 3a and 3c and using that city's temperature over the previous 10 years. We do this by multiplying the hot-side RR curve by the ratio of the linear slope before and after adaptation. This process is done separately for two age groups.

We incorporate adaptation on the cold side by scaling the cold RR slope by 18.5% of the ratio used to scale the hot RR slope (18.5% is the ratio of the hot-side to cold-side fits shown in Fig. 3). A detailed example of how adaptation is incorporated is provided in Section S3 of the supplement.

Another way we could have included adaptation is to shift the MMT toward warmer temperatures as the climate warms. This will reduce deaths due to warm temperatures, but how it affects cold mortality depends on what assumption is made for how the cold side of the RR curve evolves as the MMT shifts. If one just translates the RR curve as the MMT shifts, then cold mortality increases, largely offsetting the benefits of reduced warm mortality. Other assumptions are of course possible. Since we don't know what the best assumption is, we decided to not adjust the MMT as the climate warms. In the end, our preliminary calculations suggest that this decision does not impact the conclusions of the paper.

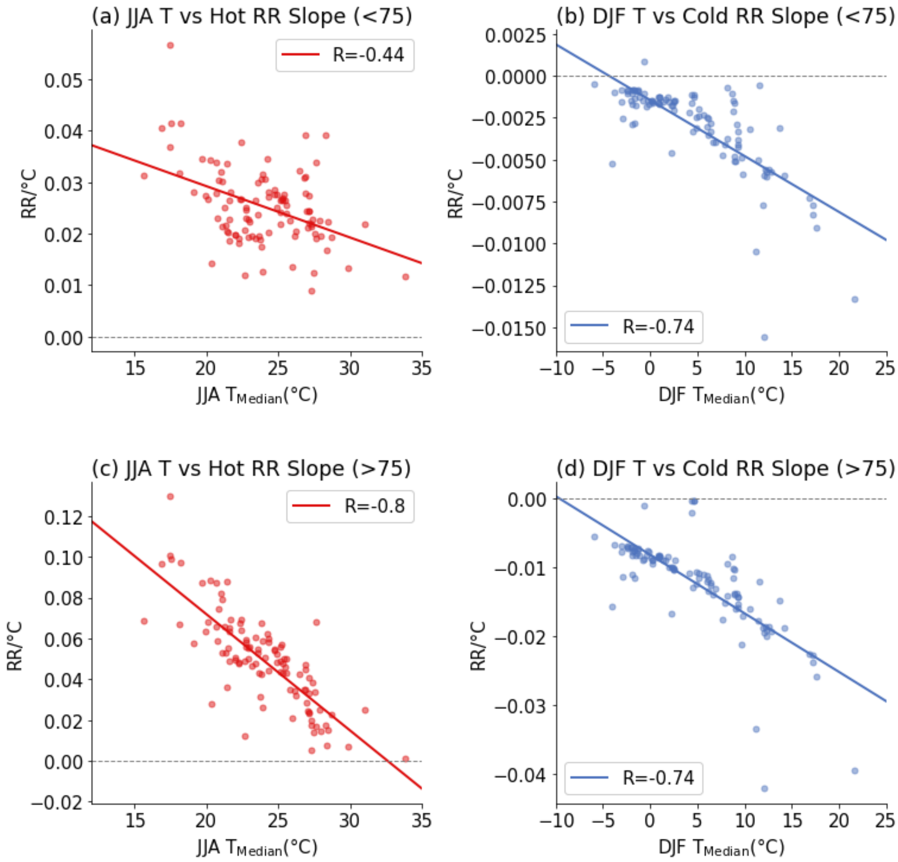

Figure 3. Relationship between the slope of each city's RR curve and that city's climate. (a) Relationship between slope of RR curve above MMT (hot RR slope) for under 75 age groups and the JJA median daily temperature. The points represent individual cities, and the line is a linear regression fit. (b) Same as (a), but for slope of RR curve below MMT (cold RR slope) and the median DJF temperature. (c, d) Same as (a, b), but for over 75 age groups.

5. Future Temperature-Related Deaths

For our projection of future temperature-related mortality, we utilize historical and RCP 8.5 scenario runs from NA-CORDEX (Mearns et al., 2017), which contain bias-corrected outputs of regional climate model (RCM) runs over North America, using boundary conditions from global climate models (GCM). Twelve combinations of GCMs and RCMs are used in this study, and these are summarized in Table 1. Historical simulations cover the period from 1950 to

2005 and RCP 8.5 simulations cover 2006 to 2099. Bias-corrected NA-CORDEX temperature only has daily maximum and daily minimum temperatures, so daily average temperature is calculated by averaging those. NA-CORDEX data are in 0.22°×0.22° horizontal resolution, so the 4 grid points nearest to each city are used to represent the temperature of the city.

Table 1. Description of NA-CORDEX members used in this study.

Scenario	Global Climate Model	Regional Climate Model	Bias-Correction
Historical + RCP 8.5	CanESM2	CanRCM4	MBCn using Daymet
		CRCM5-UQAM	
	GEMatm-Can	CRCM5-UQAM	
	GEMatm-MPI	CRCM5-UQAM	
	GFDL-ESM2M	RegCM4	
		WRF	
	HadGEM2-ES	RegCM4	
		WRF	
	MPI-ESM-LR	CRCM5-UQAM	
		RegCM4	
		WRF	
	MPI-ESM-MR	CRCM5-UQAM	

We validate the NA-CORDEX ensemble by predicting temperature-related deaths in 1987-2000 period. We do this by plugging temperatures from the NA-CORDEX ensemble for each city over that period into that city's regression model. The average number of temperature-related deaths estimated using NA-CORDEX temperatures is 36,675 (inter-model 95% CI = 36,189 – 37,231), in which 5,067 (95% CI = 4,666 – 5,332) deaths are heat-related, and 31,608 (95% CI = 31,111 – 32,331) are cold-related. Using ERA-5 temperatures, we estimated 36,444, 4,819, and 31,625 deaths, respectively. This provides some confidence in the NA-CORDEX temperature fields.

For future temperature-related mortality predictions, we also need predictions of population and demographics. For this, we use the SSP5 scenario, a fossil-fueled development scenario, which is usually paired with the RCP8.5 emissions. We use data from Hauer (2019), which contains county-level estimates of population and demographics at 5-year intervals from 2020 to 2100. To convert the county-level estimate to the city level, we extract counties containing each city in our analysis. 74% of the cities are within 1 county, and for these we assume that the city's population remains a constant fraction of the county's population. For cities that are in multiple counties, we sum the population of all counties that include the cities. Because the counties and city do not perfectly overlap, we take historical demographic data from 2020 and SSP5 data from 2020 and estimate the fraction of the total counties' population living in the city, and assume that fraction is constant over the century. From this, we come up with time series of population estimates in two age groups for each city in the coming century. A summary of population and demographic projections, as well as sensitivity due to choice of socioeconomic pathways can be found on the Supplement section S4.

To estimate future deaths, we plug NA-CORDEX temperatures for the 21^{st} century for each city into that city's regression model (Fig. S1) and then use population and demographic information to convert RR to temperature-related mortality numbers.

RCP8.5 emissions will likely exceed actual emissions, so we plot estimated mortality as a function of global average surface temperature (relative to the 1850-1859 period). We take global average warming in each year of the CORDEX-NA from averages of the four global climate models included in CORDEX-NA: CanESM2 (5 ensemble members) (Chylek et al., 2011), GFDL-ESM2M (1 run) (Dunne et al., 2020), HadGEM2-ES (3 ensemble members) (Collins et al., 2011) and MPI-ESM (100 ensemble members) (Maher et al., 2019) with historical and RCP 8.5

forcing. We first average the ensemble members of each climate model and then average those to come up with the final global average temperature time series. This gives us the global average warming of 0.83°C in 2000 and 1.37°C in year 2022, close to observed values.

With future climate projections from NA-CORDEX, future population and demographics projection from SSP5, and our two adaptation scenarios, we calculate future temperature-related mortality (Fig. 4a-d). Looking at total temperature-related deaths and no adaptation, we find that there are 45,800 deaths annually between 2011-2020 (1.16°C warming) and that is projected to grow to 200,000 with 3°C of global average warming, with both heat- and cold-related deaths increasing (Fig. 4a and 4b). There are 12,500 deaths due to significant temperatures (Fig. 4c, 4d), which is projected to increase to 63,000 at 3°C, a proportionally larger increase than all-temperature deaths. Adaptation will decrease this number, reducing the increase of temperature-related mortality at 3°C by about 28%.

We now decompose the increase in temperature-related mortality into contributions from climate change, demographics change, and population change. To estimate the impact of each of these terms, we repeat the mortality calculation with that term fixed and then subtract the values obtained from the calculation with all terms varying.

To estimate the impact of climate change, we fix climate by repeating the daily temperature of recent years (2011-2020) for the entire period (1987-2100) and then subtracting the resulting temperature-related mortality from the all-factor calculation. For the no-adaptation case, lives saved by less cold balances the lives lost due to more hot temperatures until about 3°C. Above that, the increase in heat-related mortality overwhelms and total mortality rises rapidly. For the adaptation scenario, temperature-related mortality decreases at all temperatures.

We also find that temperature-related mortality in response to the most significant temperatures will increase at all levels of warming (Fig. 4g-h). This tells us that most of the lives saved in a warming world is due to a reduction in moderate cold temperatures.

Next, we look at impact of demographics (Fig. 4i-l) by performing a fixed-demographics calculation that fixes the ratio of under/over 75 population to the 2011-2020 average and then subtracting this from the all-factor calculation. We find that the aging of our population drives an enormous increase in deaths (Fig. 4i) due to the older age group being more vulnerable to temperature-related mortality (Fig. 4j).

Finally, we calculate the impact of population (Fig. 4m-p) by fixing population at the 2011-2020 average value and subtracting the results from the all-factor calculation. As the population increases, the total number of deaths also increases.

Comparing the three contributing terms, we find that changes in demographics and population are the most important driver of future mortality, and then climate change. This likely reflects the enormous investments in adaptation that have already been made (e.g., nearly 100% air conditioner penetration in cities like Phoenix and Houston). It seems certain that poorer countries are experiencing more temperature-related mortality today and will experience even more as the climate warms in the future (Carleton et al., 2022).

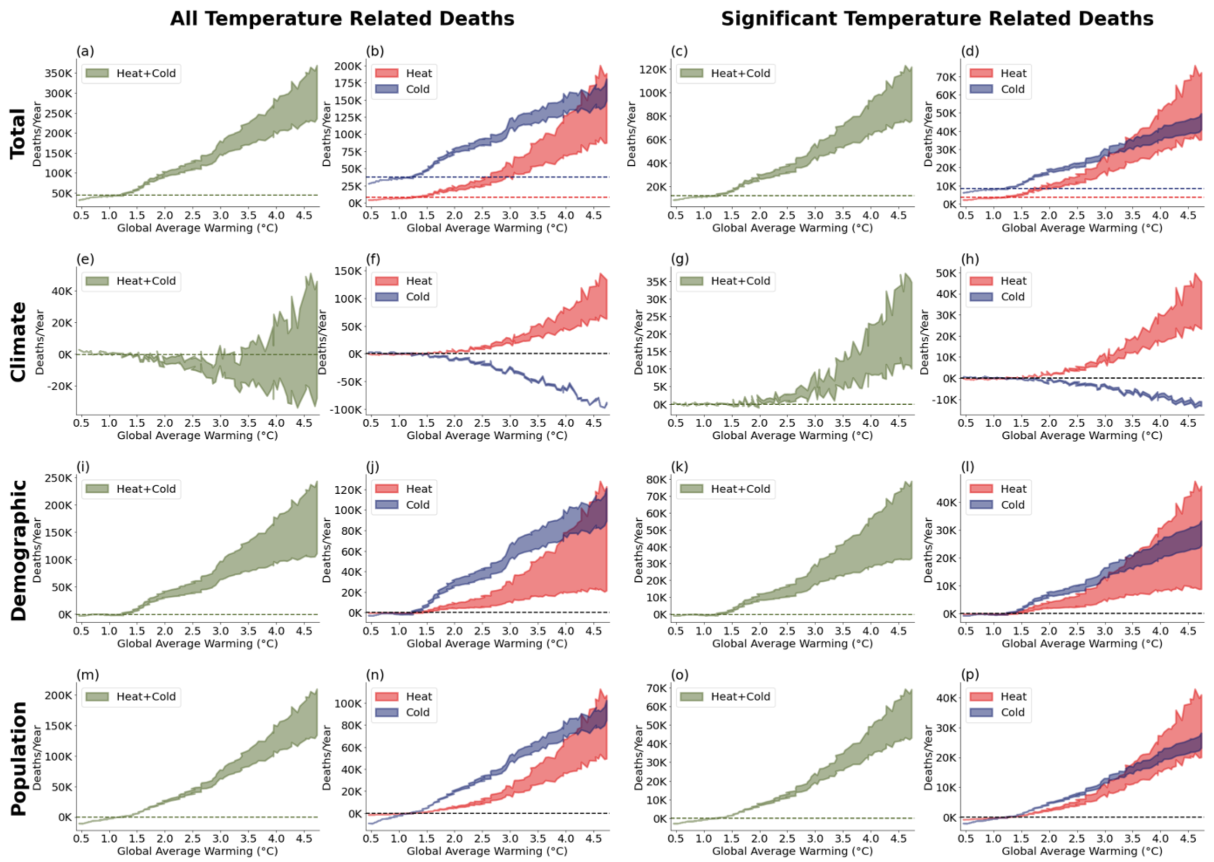

Figure 4. Estimates of future temperature-related deaths as a function of global average warming. (a-d) Future temperature-related deaths incorporating all factors: climate, demographics, and population. Upper limit of shaded region represents no-adaptation scenario, while the lower limit represents the adaptation scenario. (a) All temperature related mortality, (b) heat- and cold-related deaths, (c) mortality due to significant temperatures, (d) mortality due to significant heat and cold. Lower rows follow the same pattern as (a-d), but considering only climate change (e-h), demographics change (i-l) and population change (m-p). In all panels, dashed lines represent the average of the current value (2011-2020).

6. The Spatial Pattern of Temperature-Related Deaths

We now analyze the spatial distribution of heat-related mortality. We focus on the meridional variations in number of deaths at 3°C global average warming, approximately business-as-usual warming for 2100. We find that most of the temperature-related deaths occur between 40°N and 45°N (Fig. 5a). Analyzing per capita deaths, we find they are also weighted towards higher latitudes (Fig. 5c).

Looking at the climate contribution (Fig. 5e and 5g), we see that climate change shifts mortality poleward. This occurs because Southern cities in the U.S. are already well adapted to heat (Fig. 3), so further warming does not add significantly to heat-related deaths. However, these Southern cities do experience a decline of cold-related deaths, leading to a net reduction in temperature-related mortality. Northern cities, on the other hand, are less adapted to heat, so they experience large increases in heat-related mortality, which exceeds the decline in cold-related mortality.

The impact of adaptation is particularly pronounced between 30°N-35°N (Fig 5e) due to demographics. Currently, the 30°N-35°N region is the second youngest region (percentage of over 75 age group = 5.29%); when the Earth reaches 3°C of global average warming, it will be the oldest region (17.32%). Since the older age group is both more vulnerable to high temperatures and more sensitive to adaptation (Fig. 3), adaptation will have a large impact on mortality over this latitude range.

We have made similar plots for significant heat- and cold-related deaths (mortality in the hottest and coldest 30 days), and they show a stronger impact from climate change (Fig. S5). Numbers for all temperature-related deaths at 3°C warming are tabulated in Section S6 of the supplement.

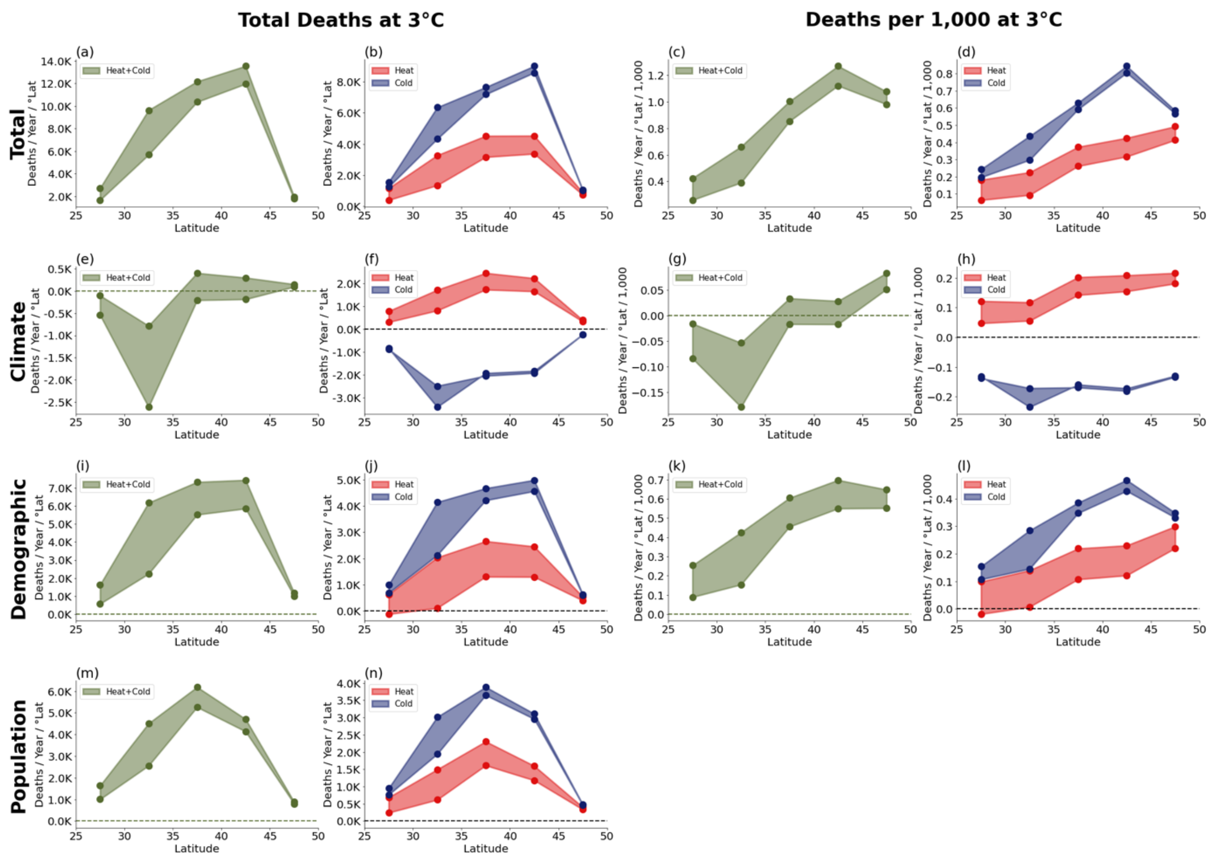

Figure 5. Meridional distribution of temperature-related deaths in 3°C world. (a) Number of temperature related deaths in 3°C world. The upper limit of the shaded region represents no-adaptation scenario, while the lower limit represents the adaptation scenario. (b) Same as (a), but for heat- and cold-related deaths. (c, d) Same as (a, b), but per capita (each bin has been divided by population in that bin). (e-h) Contribution of climate change to mortality, (i-l) contribution of demographic changes to mortality, (m-n) contribution of changes in population.

7. Conclusions

In this paper, we use mortality and temperature data obtained between 1987 and 2000 to develop a temperature-mortality relationship for 106 cities in the U.S. covering about 65% of the total population. We then use the regression models with temperatures from an ensemble of high-resolution climate simulations to estimate future temperature-related deaths. Because of the key role of adaptation, we make two different adaptation scenarios: a scenario with no adaptation and what we consider to be an aggressive adaptation scenario that follows the observed variations in adaptation between cities with different climates. We also incorporate estimates of changing population and its age distribution.

We estimate that there was an average of 36,444 temperature-related deaths per year during the period 1987-2000 in the cities in our data set. Consistent with previous work (Berko, 2014; Gasparrini, Guo, Hashizume, Kinney, et al., 2015; Gasparrini et al., 2017; Heutel et al., 2021), we find that 86% of these deaths were cold-related. Most of the cold-related deaths took place at moderate temperatures just below the minimum mortality temperature (MMT), typically around 20°C, so they are categorized as cold related even though many would consider the temperatures to be mild.

We project that, with a warming climate and an increasing and aging population, temperature-related deaths will reach 200,000 per year at 3°C of global average warming without adaptation. Assuming effective adaptation reduces the increase of this number of temperature-related deaths at 3°C of warming by 28%.

By decomposing mortality into climate, demographics, and population factors, we find that demographic shifts, primarily the aging of the population, and increasing population – will be the biggest drivers of increased temperature-related mortality. Climate change will cause small changes in mortality below 3°C of global average warming due to offsetting decreases in cold-related mortality and increases in heat-related deaths. Above 3°C, the result depends on the level of adaptation with increases in heat-related deaths dominating without adaptation. Without adaptation, total mortality rises rapidly; with adaptation, mortality declines.

While changes in temperature-related mortality due to climate change may be small below 3°C, there is a meridional shift of mortality, with deaths shifting from the South to the North

(Fig. 5g-5h). Since Southern cities in U.S. are already well adapted to heat, additional warming does not add a significant number of deaths. However, Northern cities are not well adapted to heat, so heat-related mortality increases there dominate decreases in cold-related mortality.

Ultimately, no one knows how effectively we will adapt to the warmer temperatures of the coming century. However, the investments society has made to make cities like Houston or Phoenix livable in a hot climate are massive and it is far from assured that we will make similar investments in other cities as the climate warms. Many adaptive responses (e.g., installing air conditioning, improved health care, better urban planning) are too expensive for poorer individuals or communities, so adaptation will necessarily require society to pay for much of the adaptation. This would represent a huge transfer of wealth from richer to poorer members of our society, a dicey proposition in today's political environment.

There are important limitations to our analysis. First, our analysis covered 106 large cities in the U.S., so we can't reach any conclusions about rural populations of the U.S. population or Northern states that are not included in the mortality dataset (MT, ID, WY, ND, and SD). Second, we also cannot comment on the future of heat-related mortality in the rest of the world. However, given the wealth of the U.S., our present levels of adaptation are higher than in many poorer countries and our ability to enhance our adaptation is also higher. Thus, it seems likely that heat-related mortality will be a more significant problem in the rest of the world as climate change progresses through the century (Carleton et al., 2022).

Acknowledgments: This work was supported by NSF Grant AGS-1841308 to Texas A&M University.

Supplementary Material

Future Temperature Related Deaths in the US: the Impact of Climate Change and Adaptation

S1. Distributed Lag Non-linear Model (DLNM) – Model Specification and Sensitivity

The DLNM setup in this study follows a framework from previous studies form Gasparrini et al (Gasparrini, Guo, Hashizume, Kinney, et al., 2015; Gasparrini, Guo, Hashizume, Lavigne, et al., 2015). All calculations are done with the R packages *dlnm* and *mvmeta*.

S1.1. First stage model

In the first stage, the location and the age-specific temperature-mortality relationship is derived using a generalized linear model with a quasi-Poisson family. We use the following equation in this model:

$$log\left(Death_{c,a}\right) = cb(tMean_c, lag = 21) + DOW + ns(DOY) + ns(Year) \qquad (1)$$

Where $Death_{c,a}$ represents number of daily deaths in city *c* and age group *a*. $cb(tMean_c, lag = 21)$ is a cross basis function of temperature in city *c*, with up to 21 days of lag, which is obtained by the two equations of exposure-response relationship and lag-response relationship between temperature and mortality (Gasparrini, 2014). In this study, we select a cross-basis composed of quadratic B-spline with three internal knots placed at the 10^{th}, 75^{th}, and 90^{th} percentiles of the location-specific temperature. An indicator of day of week (*DOW*) is included for the weekly cycle. A natural cubic B-spline with 8 degrees of freedom for day of year is included to control the seasonal cycle (*ns(DOY)*), and a natural cubic B-spline with 1 degree of freedom per decade is included for the long-term trend (*ns(Year)*).

The association of overall temperature-mortality relationship from eq. 1 is reduced to the cumulative relationship between temperature and mortality with the function *crossreduce*, included in *dlnm*.

S1.2. Second stage model

The multivariate meta-analysis model (Gasparrini & Armstrong, 2013; Gasparrini et al., 2012) is used for the meta-analysis. It is difficult to extract the temperature-mortality relationship from some of the cities with small number of populations, due to high signal-to-noise ratio of daily deaths. Multivariate meta-analysis allows the temperature-mortality relationship in small cities to share the information of temperature-mortality relationship of larger cities with similar characteristics. For the characteristics for the city, we include average temperature, temperature range (75^{th} percentile – 25^{th} percentile), and latitude of each city (Gasparrini & Armstrong, 2011; Gasparrini, Guo, Hashizume, Kinney, et al., 2015; Gasparrini, Guo, Hashizume, Lavigne, et al., 2015). Package *mvmeta* is used for this analysis, and technical details of this analysis can be found in Gasparrini and Armstrong (2013).

S1.3. Calculation of excess deaths due to temperature

Cumulative risk ratio (RR) is calculated as a sum of RR in all lags (up to 21 days). This returns a cumulative RR relative to the mortality at minimum mortality temperature (MMT; Fig. 1 in main text and Fig. S1). Baseline deaths per thousand (baseline DPT) at the MMT is calculated by averaging the DPT values for the days within 0.5°C of MMT. From this, we can calculate DPT values at each day by multiplying cumulative RR to base DPT. We then calculate the number of excess deaths due to temperature by multiplying excess DPT by population.

S1.4. Sensitivity analysis

We tested the sensitivity of our results to the selection of parameters in the DLNM. The number of degrees of freedom to account for seasonality (dfSeas) was modulated from 7 to 9 (current value=8), and the number of degrees of freedom to account for the long-term trend (dfTrend) was modulated from 1 to 2 (current value=1). Table S1 shows the percent change of number of deaths caused by this modulation, calculated for each city. Overall, the choice of parameters changes excess deaths by less than 8%.

JJA

	dfSeas=7	dfSeas=8	dfSeas=9
dfTrend=1	1.76 (3.95)	0	0.02 (3.21)
dfTrend=2	1.86 (4.10)	-0.08 (0.08)	-0.10 (3.26)

DJF

	dfSeas=7	dfSeas=8	dfSeas=9
dfTrend=1	4.19 (8.84)	0	-7.55 (5.06)
dfTrend=2	4.81 (8.60)	0.52 (0.84)	-6.92 (4.47)

Table S1. Percent change of number of deaths due to sensitivity analysis. Percent changes are calculated for each city and average percent changes are shown in the table, while the inter-city standard deviation is shown in parentheses.

S1.5. Impact of Ozone

High Ozone (O_3) concentration is known to impact human health (Ren et al., 2008). However, O3 is also known to be correlated with temperature, especially in summertime (Porter & Heald, 2019), so it is difficult to distinguish the impact of O_3 and temperature on number of deaths. In that context, we tested if prediction errors of the DLNM (residuals) correlated with O_3 concentration.

In cities that average more than 20 daily deaths (24 cities), we calculate the prediction residual and regress against O_3 concentration. Annually, the p value of this regression is 0.58 (inter-city standard deviation $1\sigma=0.28$). For JJA, the p value is 0.48 ($1\sigma=0.29$), showing no significant correlation between the prediction residual and O_3 concentration.

Since the effect of O_3 could be non-linear, we computed the composite analysis between the residuals on the high O_3 days (over 75th percentile of O_3) and low O_3 days (under 25th percentile of O_3). In a t-test comparing the means of the annual values, the p value is 0.59 ($1\sigma=0.27$). When comparing only JJA, the p value is 0.48 ($1\sigma=0.30$), showing that there is no significant difference of the prediction residuals on high O_3 days vs. low O_3 days.

With this analysis, we see no evidence that our results are impacted by O_3. However, given the high collinearity between temperature and O_3, we cannot rule out some contribution to mortality from O_3. Clearly, more work on this is warranted.

S2. RR Curve for Populated Cities.

Fig. 1 in main text shows the RR values that are averaged for all cities. Fig. S1 shows the RR curves for the 25 most populated cities.

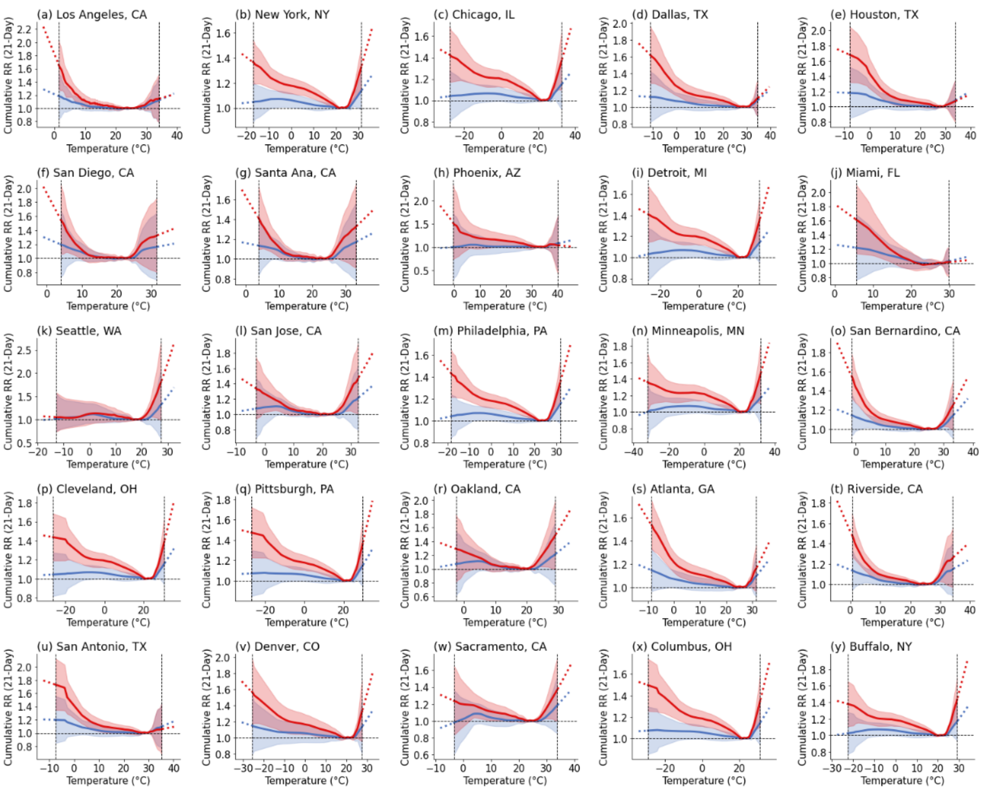

Figure S1. RR curve for 25 most populated cities. The red line represents the RR for the over 75 age group and the blue line represents the under 75 group. Solid lines are for historical temperature range, and dashed line are extrapolated RR values for the temperature outside the historical observations. Shaded regions show the 95% confidence interval of RR curve.

S3. Measuring and Applying Adaptation – Example of New York

For a more detailed explanation of measuring adaptation, here we go through an example of how we apply adaptation in our analysis. We select the >75 old age group in the city of New York City (NYC) in this example, but same process is applied for all age groups and all individual cities.

Fig. S2a shows that, in the 1987-2000 period, ERA-5 median JJA temperature in NYC was 22.7°C. From the projections of CORDEX-NA, median JJA temperature rises to 25.6°C in a world with 3°C global average warming.

In the 1987-2000 period, the hot-side RR slope of NY is 0.0491 (RR/°C) (blue dashed line and blue dot in Fig. S2b). As seen in Fig. S2c, the RR curves are not linear, but the linear fit gives us a metric for how steeply the curve rises.

Using the slopes of the linear fits computed from all cities, we find that the hot side RR slope changes by -0.0057 (RR/°C/°C) as JJA median temperature increases (Fig. 3c in the main text, gray dashed line in Fig S2b). Using the increase in JJA median temperature for NYC, we therefore estimate that the hot-side RR slope of NY would decrease to 0.0296 (RR/°C) in a 3°C warmer world (red dashed line and red dot in Fig. S2b).

The last step is to adjust the RR curve by multiplying the hot-side mortality curve by the ratio of hot-side RR slope of 1987-2000 to that in 3°C world (0.0322/0.0491). This gives the RR curve in 3°C world (red line above the MMT in Fig. S2c). For the cold-side RR curve, the mortality curve is decreased by 18.5% of the ratio of the hot-side RR curve (red line below the MMT Fig. S2c), as discussed in the main text.

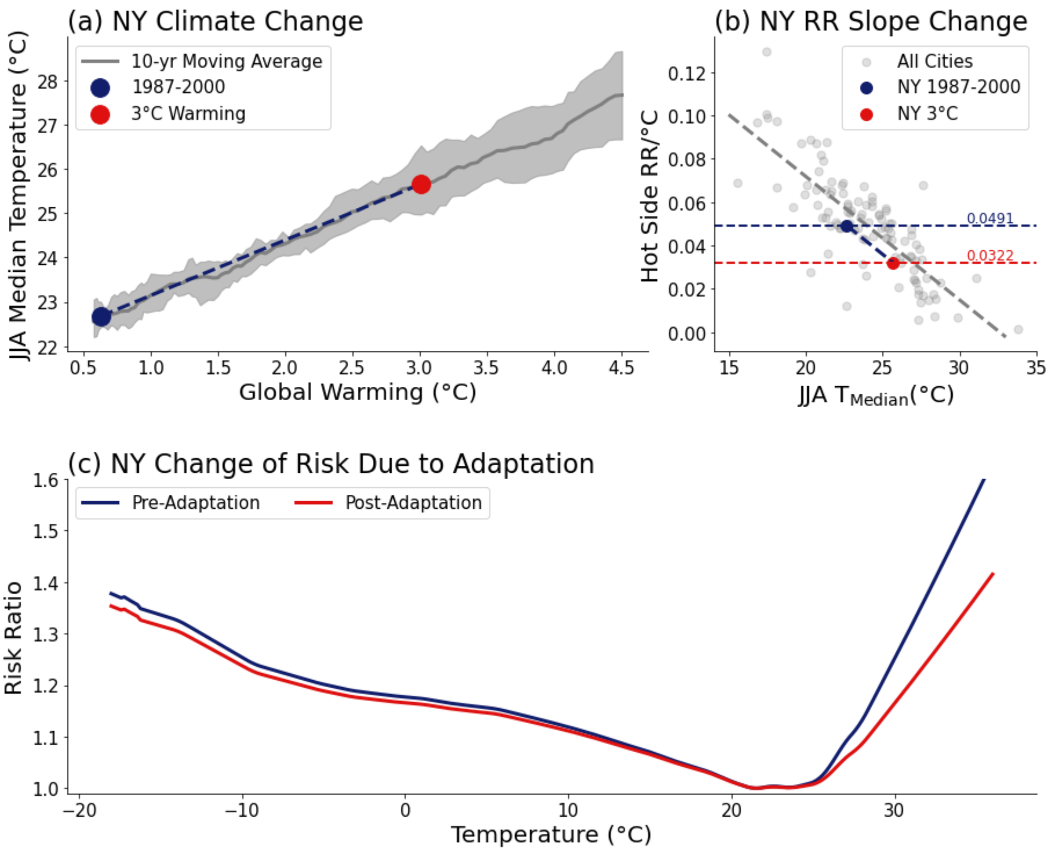

Figure S2. Example of measuring and applying adaptation, with >75 age group in New York City as example. (a) Current and future JJA median temperature. Gray shaded region is the upper and lower limit of climate projection from CORDEX-NA, and the gray solid line is the mean projection of NA-CORDEX. The values for the NA-CORDEX are smoothed with 10-yr moving average. Blue point is the 1987-2000 JJA median temperature from ERA-5, and red point is the JJA median temperature at 3°C of global warming. (b) Change of hot side RR slope with temperature. Gray points and dashed line represent the individual cities and the linear fit of those cities, same as Fig. 3c in the main text. Blue point and red point each show the hot side RR slope of NYC in 1987-2000 period and 3°C world. (c) Change of RR curve in NYC. Blue line represents the RR curve in 1987-2000 period, and red line represents the RR curve in 3°C world, when adaptation applied.

S4. Future Population Scenario

Fig. S3 summarizes the future population and demographic change. In the 106 cities used in this study, total population increases at a rate of 18.5 million/decade. The fraction of population over 75 also increases at an average rate of 1.7%/decade. Top three cities with highest population increase are Austin (TX), Denver (CO), and Raleigh (NC), wile top three cities with fastest aging population are Jackson (MS), Richmond (VA), and Santa Ana/Anaheim (CA).

Furthermore, we test the sensitivity due to future population scenario by comparing SSP2 (middle of the road) scenario with SSP5 scenario (currently used in the main text). First looking at total population, we observe a lower population increase in SSP2 scenario (Fig. S3a). This would decrease the contribution of population to total deaths (Figs. 4m-4p). The proportion of >75 age groups are very similar until year 2080 (3.3°C warming, Fig.S3b), so the contribution of changing demographics would be similar (Figs. 4i-4l), although the magnitude differs by the ratio of population in SSP5 and SSP2 (0.8 in 3°C warming). The impact of climate change (Figs. 4e-4h) is also similar with magnitude decreasing by the ratio of population in SSP5 and SSP2.

The inter-city pattern of slope of change in population and >75 age group ratio is nearly identical in SSP5 and SSP2. The R^2 of the regression between the population slope distribution (Fig. S3c shows the slopes for SSP5) between SSP5 and SSP2 is 0.999 and R^2 value of aging slope distribution (Fig. S3d) is 0.996.

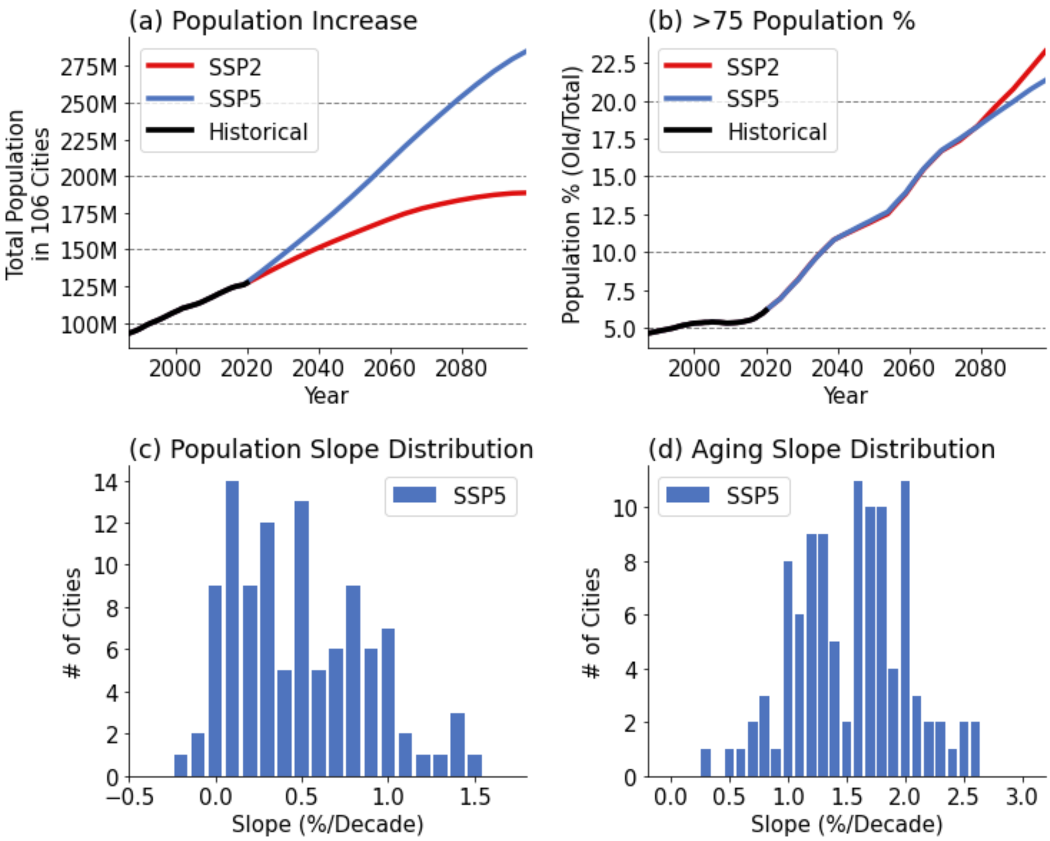

Figure S3. Summary of future population and demographic change. (a) Change of total population for all 106 cities in SSP2 and SSP5 scenarios. (b) Change in fraction of > 75 population, calculated by adding all > 75 population over 106 cities and dividing by total population. (c) Distribution of population trends of individual cities in the SSP5 scenario, relative to average historical population (1987-2020). (d) Distribution of growth of the fraction of the > 75 age group, in the SSP5 scenario.

S5. Meridional Distribution of Significant Temperature Related Deaths

Here we show the plot same as Fig. 5, but using significant temperature related deaths, which is deaths in 30 days each year with the highest and lowest temperatures.

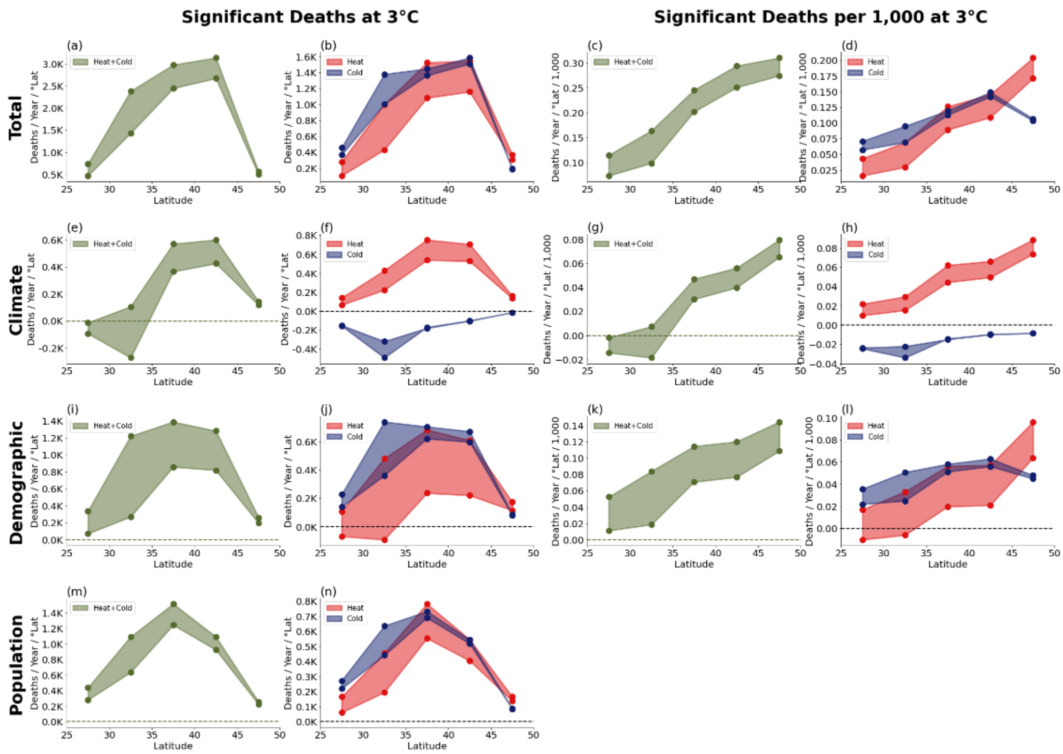

Figure S4. Meridional distribution of significant temperature-related deaths in 3°C world, where significant refers to the deaths in 30 days of the year with the highest and lowest temperatures. (a) Number of deaths in 3°C world. Upper limit of the shaded region represents no-adaptation scenario, while the lower limit represents the adaptation scenario. (b) Same as (a), but for heat- and cold-related significant deaths. (c, d) Same as (a, b), but per capita (each bin has been divided by population in that bin). (e-h) Contribution of climate change to mortality, (i-l) contribution of demographic changes to mortality, (m, n) contribution of changes in population.

S6. Future predictions of Temperature Related Deaths

Table S2 shows the values of total projected deaths including all factors at 3°C global average warming as well as our estimate of deaths just due to climate change. Table S3 shows the same thing for significant temperatures.

Table S2. The number of temperature related deaths in each city at 3°C warming, and number of deaths caused by climate change. XA = excluding adaptation, OA = with adaptation. Negative numbers indicate a reduction in mortality at 3°C. Shading in the table represents the magnitude of increase (red) and decrease (blue)

	Deaths						Climate Effect					
City	Heat+Cold		Heat		Cold		Heat+Cold		Heat		Cold	
	XA	OA	XA	OA	XA	OA	XA	OA	XA	OA	XA	OA
Akron, OH	713	645	244	194	468	451	13	-8	118	93	-105	-101
Albuquerque, NM	972	706	320	129	652	577	-16	-90	159	66	-176	-156

Arlington, VA	623	555	199	150	424	405	-3	-22	93	69	-96	-92
Atlanta, GA	3080	2633	972	653	2109	1980	-75	-215	546	368	-621	-583
Austin, TX	2255	1451	674	143	1581	1308	-316	-516	376	93	-692	-609
Bakersfield, CA	1200	971	491	311	709	660	64	-20	271	173	-207	-193
Baltimore, MD	782	716	272	223	510	493	20	-1	138	113	-118	-114
Baton Rouge, LA	309	231	113	55	195	176	-17	-42	68	35	-85	-77
Biddeford, ME	613	562	238	198	375	364	38	19	125	103	-87	-84
Birmingham, AL	612	496	207	123	404	373	-1	-41	124	74	-125	-115
Boston, MA	2214	1993	837	667	1376	1326	98	21	427	338	-329	-317
Buffalo, NY	1536	1413	567	472	969	940	87	43	293	243	-207	-200
Cayce, SC	413	330	141	81	272	250	-10	-34	72	42	-82	-75
Cedar Rapids, IA	648	565	203	144	445	421	2	-20	92	65	-90	-85
Charlotte, NC	2658	2286	903	630	1754	1656	5	-114	479	333	-474	-447
Chicago, IL	8665	7827	2531	1949	6134	5878	-98	-329	1213	926	-1311	-1255
Cincinnati, OH	1042	921	347	259	695	662	12	-25	172	128	-160	-153
Cleveland, OH	1456	1348	468	390	988	958	15	-18	235	195	-220	-213
Columbus, GA	305	259	113	78	192	181	8	-9	70	49	-62	-58
Columbus, OH	3511	3126	1161	879	2351	2247	11	-101	548	412	-537	-513
Colorado Springs, CO	1833	1653	907	756	926	897	316	225	603	502	-286	-277
Corpus Christi, TX	327	228	187	104	140	124	21	-21	132	78	-111	-99
Coventry, RI	204	180	72	54	132	126	7	-1	38	28	-30	-29
Dayton, OH	528	471	181	140	346	331	9	-9	89	68	-80	-77
Washington, DC	2346	2109	772	599	1574	1509	8	-61	371	286	-363	-348
Denver, CO	8438	7269	3648	2713	4790	4556	1093	564	2293	1706	-1200	-1142
Des Moines, IA	1443	1253	450	316	993	937	2	-50	217	152	-214	-202
Detroit, MI	1555	1376	486	359	1069	1017	14	-35	220	162	-207	-197
Dallas/Fort Worth, TX	7806	5467	2411	792	5395	4675	-332	-1071	1472	516	-1804	-1587
El Paso, TX	818	532	194	35	625	497	-118	-173	81	19	-199	-192
Evansville, IN	333	282	115	78	218	204	10	-6	61	41	-51	-47
Fresno, CA	1472	1198	595	380	877	819	79	-18	304	192	-225	-210
Fort Wayne, IN	816	706	277	195	540	511	4	-26	124	87	-120	-113
Grand Rapids, MI	1835	1647	653	512	1182	1136	60	5	296	231	-235	-226
Greensboro, NC	981	862	348	259	633	603	13	-25	180	134	-167	-159
Houston, TX	5956	3763	1985	460	3971	3303	-770	-1387	1154	298	-1924	-1685
Huntsville, AL	740	629	238	159	501	470	-2	-39	140	94	-142	-133
Indianapolis, IN	1770	1536	592	422	1177	1115	9	-58	281	199	-272	-257
Jackson, MS	368	283	123	62	244	221	-12	-40	72	37	-85	-77
Jacksonville, FL	963	776	451	297	512	479	67	-19	303	202	-237	-221
Jersey City, NJ	1622	1433	561	420	1061	1013	35	-23	269	200	-234	-223
Johnstown, PA	89	81	33	27	56	55	4	1	16	13	-13	-12
Kansas City, MO	2175	1926	729	548	1446	1378	67	-22	423	318	-356	-339
Kansas City, KS	324	287	111	84	213	203	13	0	66	50	-53	-50
Kingston, NY	231	213	84	70	147	143	8	2	40	33	-32	-31
Knoxville, TN	732	649	265	203	467	446	30	-1	153	117	-123	-118
Los Angeles, CA	7391	4216	2581	369	4810	3848	-1894	-2435	1005	203	-2900	-2638
Lafayette, LA	439	304	160	59	279	244	-29	-72	95	38	-125	-109
Las Vegas, NV	6564	4997	1974	906	4591	4091	36	-369	974	467	-938	-837

Lexington, KY	653	558	221	151	433	407	6	-24	113	77	-108	-101
Lincoln, NE	779	646	246	153	533	493	10	-28	125	78	-115	-107
Lake Charles, LA	261	181	93	35	168	146	-18	-43	59	24	-77	-68
Louisville, KY	1498	1286	498	343	1000	943	9	-57	254	175	-245	-231
Little Rock, AR	569	452	175	93	394	359	-3	-41	105	57	-108	-98
Lubbock, TX	409	285	133	45	277	240	-26	-60	72	26	-98	-86
Madison, WI	1435	1279	447	336	988	942	-7	-45	188	141	-195	-186
Memphis, TN	1333	1147	462	325	870	822	51	-20	286	201	-235	-221
Miami, FL	1365	468	979	221	386	246	195	-391	785	189	-590	-580
Milwaukee, WI	1526	1349	460	335	1066	1014	18	-38	237	170	-218	-207
Minneapolis/St. Paul, MN	4752	4320	1403	1105	3349	3216	34	-73	610	480	-576	-553
Mobile, AL	302	227	119	62	183	165	2	-28	80	42	-77	-70
Modesto, CA	728	638	299	227	429	411	33	-1	161	122	-128	-123
Muskegon, MI	548	511	196	168	352	343	37	22	115	98	-78	-76
Nashville, TN	1553	1342	541	385	1012	957	44	-31	313	223	-268	-254
Newport News, VA	255	220	100	72	155	147	10	-3	54	39	-45	-42
New Orleans, LA	1532	1383	694	573	838	810	137	61	513	424	-375	-363
Norfolk, VA	327	287	129	97	198	189	14	-1	72	55	-58	-55
Newark, NJ	2122	1876	735	551	1388	1324	47	-29	353	264	-306	-292
New York, NY	18954	16245	6440	4439	12513	11805	381	-458	3164	2168	-2783	-2626
Oakland, CA	1589	1389	865	689	725	700	13	-65	450	356	-436	-421
Oklahoma City, OK	1615	1270	528	282	1087	988	6	-109	318	175	-312	-284
Olympia, WA	642	584	289	241	353	343	21	3	116	96	-95	-92
Omaha, NE	1534	1315	475	322	1059	993	14	-49	239	163	-226	-212
Orlando, FL	1423	1119	803	538	621	582	237	67	603	410	-367	-343
Philadelphia, PA	2795	2484	998	764	1797	1719	91	-8	491	376	-401	-384
Phoenix, AZ	9961	1098	2139	360	7822	738	-1076	-7074	684	171	-1760	-7245
Pittsburgh, PA	1646	1501	572	463	1074	1037	32	-13	275	221	-243	-234
Portland, OR	2855	2569	1270	1034	1585	1534	128	44	490	395	-363	-351
Providence, RI	971	842	348	250	623	592	36	-8	178	127	-142	-135
Raleigh, NC	2992	2573	1070	755	1923	1818	9	-120	537	380	-528	-499
Richmond, VA	1160	1015	420	311	739	704	16	-29	205	152	-189	-180
Riverside, CA	2388	1842	972	537	1416	1305	-123	-288	492	280	-615	-569
Rochester, NY	1072	993	389	329	683	664	44	15	206	173	-162	-158
Sacramento, CA	2427	2091	932	670	1494	1420	29	-81	452	320	-423	-401
Salt Lake City, UT	3578	3118	1438	1080	2140	2038	396	209	849	640	-453	-432
San Antonio, TX	2389	1291	725	170	1664	1120	-437	-848	380	116	-817	-964
San Bernardino, CA	2074	1789	775	556	1299	1233	-102	-186	396	288	-498	-474
San Diego, CA	2133	1385	1434	742	700	642	162	-213	922	486	-760	-699
San Francisco, CA	535	452	426	347	108	105	125	76	279	225	-154	-150
San Jose, CA	1728	1516	691	522	1037	994	-266	-310	257	191	-523	-501
Seattle, WA	2931	2732	1436	1267	1495	1465	284	210	670	588	-386	-378
Shreveport, LA	298	219	93	38	205	181	-16	-40	56	24	-72	-64
Spokane, WA	1592	1418	668	530	924	888	199	139	331	266	-132	-127
Santa Ana/Anaheim, CA	2211	1671	1251	774	960	897	-73	-288	707	442	-780	-730
St. Louis, MO	710	627	231	172	479	455	13	-14	124	92	-111	-106

Stockton, CA	933	829	404	320	529	509	35	-4	211	166	-176	-170
St. Petersburg, FL	736	466	375	148	362	318	50	-87	285	119	-235	-205
Syracuse, NY	611	549	236	188	375	361	29	8	113	89	-84	-81
Tacoma, WA	1706	1556	783	660	922	897	114	63	347	290	-233	-227
Tampa, FL	1407	986	756	396	651	590	178	-48	572	308	-394	-356
Toledo, OH	505	439	162	115	343	325	3	-15	72	51	-70	-66
Topeka, KS	225	193	78	55	147	138	9	-3	45	32	-37	-35
Tucson, AZ	456	232	114	25	342	207	-57	-150	43	13	-100	-164
Tulsa, OK	1373	1104	480	282	893	822	47	-55	301	178	-254	-234
Wichita, KS	871	684	287	152	583	531	22	-44	169	90	-147	-134
Worcester, MA	1164	1035	396	301	768	735	24	-15	181	136	-158	-151

Table S3. The number of significant temperature related deaths in each city at 3°C warming, and number of significant temperature related deaths caused by climate change.

	Deaths						Climate Effect					
City	Heat+Cold		Heat		Cold		Heat+Cold		Heat		Cold	
	XA	OA	XA	OA	XA	OA	XA	OA	XA	OA	XA	OA
Akron, OH	212	187	103	83	108	104	38	29	46	37	-8	-8
Albuquerque, NM	288	190	135	55	152	135	31	0	58	23	-27	-24
Arlington, VA	182	158	82	62	100	95	27	19	35	26	-8	-7
Atlanta, GA	956	796	400	273	556	522	111	56	195	135	-84	-79
Austin, TX	708	446	234	53	474	393	-32	-81	87	28	-120	-109
Bakersfield, CA	406	312	223	142	183	170	87	48	112	72	-25	-24
Baltimore, MD	241	216	120	99	121	117	48	38	58	48	-10	-10
Baton Rouge, LA	99	75	35	18	64	57	1	-4	15	8	-14	-13
Biddeford, ME	197	176	110	92	86	84	50	41	56	47	-6	-6
Birmingham, AL	188	148	80	49	108	100	24	10	40	25	-16	-15
Boston, MA	690	604	369	294	321	310	155	119	178	141	-23	-22
Buffalo, NY	476	427	261	218	215	209	117	95	131	109	-14	-14
Cayce, SC	126	98	52	31	73	68	12	4	21	13	-9	-8
Cedar Rapids, IA	184	154	85	61	99	93	31	21	36	26	-5	-5
Charlotte, NC	825	689	379	268	446	421	128	78	181	128	-53	-50
Chicago, IL	2408	2114	1066	827	1343	1287	374	275	453	351	-79	-76
Cincinnati, OH	303	261	139	104	164	156	48	33	62	47	-14	-13
Cleveland, OH	431	390	208	174	223	217	81	65	98	81	-17	-16
Columbus, GA	99	82	45	32	53	50	16	9	24	17	-9	-8
Columbus, OH	1017	882	464	354	552	528	156	110	198	150	-42	-40
Colorado Springs, CO	694	610	461	384	233	226	240	194	287	239	-47	-45
Corpus Christi, TX	117	86	57	32	60	53	5	-4	31	19	-25	-23
Coventry, RI	64	54	33	25	31	29	14	10	16	12	-2	-2
Dayton, OH	156	136	74	58	82	78	27	20	34	26	-7	-6
Washington, DC	702	615	328	256	374	359	116	85	145	113	-29	-28
Denver, CO	2877	2375	1766	1318	1110	1056	903	648	1033	771	-130	-124

Des Moines, IA	410	343	188	133	223	210	72	49	83	59	-11	-11
Detroit, MI	446	380	214	159	232	221	77	54	90	67	-13	-13
Dallas/Fort Worth, TX	2352	1551	935	321	1417	1230	188	-66	459	174	-271	-240
El Paso, TX	232	140	74	14	158	126	-12	-29	22	6	-34	-35
Evansville, IN	98	81	47	32	51	48	17	11	22	16	-5	-4
Fresno, CA	479	371	263	169	217	202	97	53	124	78	-27	-25
Fort Wayne, IN	233	195	109	78	124	117	36	23	44	31	-8	-8
Grand Rapids, MI	541	471	281	221	261	250	109	83	123	96	-14	-13
Greensboro, NC	299	256	140	105	159	151	47	32	65	49	-17	-17
Houston, TX	1878	1210	610	152	1268	1058	-134	-244	221	75	-355	-318
Huntsville, AL	223	184	95	64	128	120	32	17	49	33	-17	-16
Indianapolis, IN	510	430	234	168	276	262	78	51	99	71	-21	-20
Jackson, MS	110	83	42	22	68	62	7	0	18	10	-11	-10
Jacksonville, FL	342	278	158	106	184	172	58	31	92	63	-34	-32
Jersey City, NJ	484	413	239	180	244	233	88	62	106	79	-18	-17
Johnstown, PA	28	25	15	12	14	13	6	5	7	6	-1	-1
Kansas City, MO	661	567	326	247	335	319	155	113	180	137	-26	-24
Kansas City, KS	100	86	51	39	50	47	25	18	29	22	-4	-4
Kingston, NY	73	65	38	32	35	33	15	12	18	15	-2	-2
Knoxville, TN	230	200	111	85	119	114	45	32	59	46	-14	-14
Los Angeles, CA	2683	1517	972	147	1711	1369	-311	-482	247	59	-558	-541
Lafayette, LA	138	98	48	18	90	79	-2	-10	19	9	-21	-18
Las Vegas, NV	1836	1274	861	405	975	870	284	114	352	175	-68	-61
Lexington, KY	193	160	87	60	106	99	29	17	40	27	-11	-10
Lincoln, NE	225	177	105	66	120	111	42	25	49	31	-7	-6
Lake Charles, LA	82	58	29	12	54	47	0	-5	13	6	-13	-12
Louisville, KY	435	362	194	136	241	227	63	38	86	60	-23	-22
Little Rock, AR	171	129	73	40	98	89	25	9	38	21	-13	-12
Lubbock, TX	124	82	50	18	74	65	5	-6	21	8	-16	-14
Madison, WI	397	343	180	136	216	207	56	40	67	51	-11	-10
Memphis, TN	403	337	188	134	214	202	76	48	104	74	-27	-26
Miami, FL	582	259	263	57	319	202	-82	-232	157	37	-239	-269
Milwaukee, WI	439	372	210	154	229	218	88	60	102	74	-14	-14
Minneapolis/St. Paul, MN	1312	1156	612	484	700	672	229	177	253	200	-23	-22
Mobile, AL	97	73	39	21	57	52	10	1	21	12	-11	-10
Modesto, CA	248	211	138	105	111	106	52	36	70	53	-18	-17
Muskegon, MI	172	156	95	82	77	75	49	42	54	47	-5	-5
Nashville, TN	472	397	220	159	252	238	86	56	115	83	-29	-27
Newport News, VA	80	67	41	30	40	38	16	11	20	15	-4	-4
New Orleans, LA	461	413	235	194	226	219	118	94	145	121	-27	-26
Norfolk, VA	104	89	53	41	51	49	22	16	27	21	-5	-5
Newark, NJ	636	544	316	238	320	306	118	83	141	106	-23	-22
New York, NY	5627	4616	2759	1910	2869	2707	1032	650	1250	855	-218	-206
Oakland, CA	634	549	382	305	252	244	83	49	176	139	-93	-90
Oklahoma City, OK	487	364	218	119	269	245	77	31	114	65	-38	-34
Olympia, WA	240	212	152	127	88	85	51	41	59	49	-9	-8

Omaha, NE	438	359	202	138	235	221	82	54	94	65	-12	-11
Orlando, FL	569	462	277	189	292	273	113	61	186	129	-73	-68
Philadelphia, PA	852	734	434	334	418	400	169	124	200	153	-31	-30
Phoenix, AZ	2608	364	874	175	1734	189	10	-1336	187	72	-177	-1408
Pittsburgh, PA	493	440	237	193	256	247	88	68	108	87	-20	-19
Portland, OR	1048	912	664	541	383	371	227	177	261	210	-34	-33
Providence, RI	297	247	154	111	144	136	63	43	73	53	-10	-10
Raleigh, NC	902	756	412	293	490	463	125	76	180	128	-55	-52
Richmond, VA	352	300	169	126	183	175	57	39	75	56	-17	-17
Riverside, CA	862	639	424	235	439	404	87	8	199	112	-112	-103
Rochester, NY	331	300	175	149	156	152	78	64	89	75	-11	-11
Sacramento, CA	788	655	414	299	375	356	124	76	179	127	-54	-52
Salt Lake City, UT	1191	989	728	547	464	442	349	254	398	300	-48	-46
San Antonio, TX	782	422	251	62	530	360	-68	-184	88	34	-156	-218
San Bernardino, CA	713	599	338	243	375	356	75	35	159	115	-84	-80
San Diego, CA	1001	645	677	347	325	298	180	-1	416	215	-237	-217
San Francisco, CA	235	200	180	147	55	54	57	39	98	79	-41	-40
San Jose, CA	663	573	308	233	355	340	-4	-26	103	76	-107	-103
Seattle, WA	1147	1048	782	691	365	357	320	277	351	308	-31	-31
Shreveport, LA	91	64	35	15	56	50	6	-2	16	7	-10	-9
Spokane, WA	573	487	380	301	194	186	184	145	191	152	-7	-7
Santa Ana/Anaheim, CA	918	689	534	330	384	359	89	-5	279	173	-190	-177
St. Louis, MO	208	179	97	73	111	106	40	28	48	36	-8	-8
Stockton, CA	328	285	185	147	143	138	63	45	90	71	-27	-26
St. Petersburg, FL	285	199	112	47	173	153	17	-15	71	32	-54	-47
Syracuse, NY	189	166	103	82	87	83	42	32	48	38	-6	-6
Tacoma, WA	647	574	423	356	224	218	162	132	182	152	-20	-20
Tampa, FL	542	405	235	127	307	278	67	9	153	86	-86	-77
Toledo, OH	143	119	67	48	76	72	22	15	27	19	-5	-4
Topeka, KS	69	57	35	25	34	32	16	11	19	14	-3	-3
Tucson, AZ	127	62	43	11	84	51	-3	-26	10	4	-13	-30
Tulsa, OK	423	324	204	122	218	201	89	46	116	71	-27	-25
Wichita, KS	256	189	121	66	135	123	51	23	64	35	-13	-12
Worcester, MA	349	300	174	133	174	167	65	46	76	57	-11	-11

References

Anderson, G. B., Oleson, K. W., Jones, B., & Peng, R. D. (2018). Projected trends in high-mortality heatwaves under different scenarios of climate, population, and adaptation in 82 US communities. *Climatic change, 146*(3), 455-470,

Åström, D. O., Forsberg, B., Edvinsson, S., & Rocklöv, J. (2013). Acute fatal effects of short-lasting extreme temperatures in Stockholm, Sweden: evidence across a century of change. *Epidemiology, 24*(6), 820-829,

Barnett, A. G. (2007). Temperature and cardiovascular deaths in the US elderly: changes over time. *Epidemiology, 18*(3), 369-372,

Barreca, A., Clay, K., Deschenes, O., Greenstone, M., & Shapiro, J. S. (2016). Adapting to climate change: The remarkable decline in the US temperature-mortality relationship over the twentieth century. *Journal of Political Economy, 124*(1), 105-159,

Barreca, A. I. (2012). Climate change, humidity, and mortality in the United States. *Journal of Environmental Economics and Management, 63*(1), 19-34,

Berko, J. (2014). *Deaths attributed to heat, cold, and other weather events in the United States, 2006-2010*: US Department of Health and Human Services, Centers for Disease Control and ….

Bobb, J. F., Peng, R. D., Bell, M. L., & Dominici, F. (2014). Heat-related mortality and adaptation to heat in the United States. *Environmental health perspectives, 122*(8), 811-816,

Carleton, T., Jina, A., Delgado, M., Greenstone, M., Houser, T., Hsiang, S., Hultgren, A., Kopp, R. E., McCusker, K. E., & Nath, I. (2022). Valuing the global mortality consequences of climate change accounting for adaptation costs and benefits. *The Quarterly Journal of Economics, 137*(4), 2037-2105,

Carson, C., Hajat, S., Armstrong, B., & Wilkinson, P. (2006). Declining vulnerability to temperature-related mortality in London over the 20th century. *American journal of epidemiology, 164*(1), 77-84,

Chylek, P., Li, J., Dubey, M., Wang, M., & Lesins, G. (2011). Observed and model simulated 20th century Arctic temperature variability: Canadian earth system model CanESM2. *Atmospheric Chemistry and Physics Discussions, 11*(8), 22893-22907,

Collins, W., Bellouin, N., Doutriaux-Boucher, M., Gedney, N., Halloran, P., Hinton, T., Hughes, J., Jones, C., Joshi, M., & Liddicoat, S. (2011). Development and evaluation of an Earth-System model–HadGEM2. *Geoscientific Model Development, 4*(4), 1051-1075,

Davis, R. E., Knappenberger, P. C., Michaels, P. J., & Novicoff, W. M. (2003). Changing heat-related mortality in the United States. *Environmental health perspectives, 111*(14), 1712-1718,

de Schrijver, E., Bundo, M., Ragettli, M. S., Sera, F., Gasparrini, A., Franco, O. H., & Vicedo-Cabrera, A. M. (2022). Nationwide analysis of the heat-and cold-related mortality trends in Switzerland between 1969 and 2017: the role of population aging. *Environmental health perspectives, 130*(3), 037001,

Demoury, C., Aerts, R., Vandeninden, B., Van Schaeybroeck, B., & De Clercq, E. M. (2022). Impact of Short-Term Exposure to Extreme Temperatures on Mortality: A Multi-City Study in Belgium. *International Journal of Environmental Research and Public Health, 19*(7), 3763,

Deschênes, O., & Greenstone, M. (2011). Climate change, mortality, and adaptation: Evidence from annual fluctuations in weather in the US. *American Economic Journal: Applied Economics, 3*(4), 152-185,

Deschenes, O., & Moretti, E. (2009). Extreme weather events, mortality, and migration. *The Review of Economics and Statistics, 91*(4), 659-681,

Dimitrova, A., Ingole, V., Basagana, X., Ranzani, O., Mila, C., Ballester, J., & Tonne, C. (2021). Association between ambient temperature and heat waves with mortality in South Asia: Systematic review and meta-analysis. *Environment International, 146*, 106170,

Dunne, J., Horowitz, L., Adcroft, A., Ginoux, P., Held, I., John, J., Krasting, J., Malyshev, S., Naik, V., & Paulot, F. (2020). The GFDL Earth System Model version 4.1 (GFDL-ESM 4.1): Overall coupled model description and simulation characteristics. *Journal of Advances in Modeling Earth Systems, 12*(11), e2019MS002015,

Folkerts, M. A., Bröde, P., Botzen, W., Martinius, M. L., Gerrett, N., Harmsen, C. N., & Daanen, H. A. (2020). Long term adaptation to heat stress: Shifts in the minimum mortality temperature in the Netherlands. *Frontiers in Physiology, 11*, 225,

Fouillet, A., Rey, G., Wagner, V., Laaidi, K., Empereur-Bissonnet, P., Le Tertre, A., Frayssinet, P., Bessemoulin, P., Laurent, F., & De Crouy-Chanel, P. (2008). Has the impact of heat waves on mortality changed in France since the European heat wave of summer 2003? A study of the 2006 heat wave. *International journal of epidemiology, 37*(2), 309-317,

Gasparrini, A., & Armstrong, B. (2011). The impact of heat waves on mortality. *Epidemiology (Cambridge, Mass.), 22*(1), 68,

Gasparrini, A., Guo, Y., Hashizume, M., Kinney, P. L., Petkova, E. P., Lavigne, E., Zanobetti, A., Schwartz, J. D., Tobias, A., & Leone, M. (2015). Temporal variation in heat–mortality associations: a multicountry study. *Environmental health perspectives, 123*(11),

1200-1207,
Gasparrini, A., Guo, Y., Hashizume, M., Lavigne, E., Zanobetti, A., Schwartz, J., Tobias, A., Tong, S., Rocklöv, J., & Forsberg, B. (2015). Mortality risk attributable to high and low ambient temperature: a multicountry observational study. *The lancet, 386*(9991), 369-375,
Gasparrini, A., Guo, Y., Sera, F., Vicedo-Cabrera, A. M., Huber, V., Tong, S., Coelho, M. d. S. Z. S., Saldiva, P. H. N., Lavigne, E., & Correa, P. M. (2017). Projections of temperature-related excess mortality under climate change scenarios. *The Lancet Planetary Health, 1*(9), e360-e367,
Gosling, S. N., McGregor, G. R., & Lowe, J. A. (2009). Climate change and heat-related mortality in six cities Part 2: climate model evaluation and projected impacts from changes in the mean and variability of temperature with climate change. *International journal of biometeorology, 53*(1), 31-51,
Guo, Y., Barnett, A. G., Pan, X., Yu, W., & Tong, S. (2011). The impact of temperature on mortality in Tianjin, China: a case-crossover design with a distributed lag nonlinear model. *Environmental health perspectives, 119*(12), 1719-1725,
Hajat, S., Vardoulakis, S., Heaviside, C., & Eggen, B. (2014). Climate change effects on human health: projections of temperature-related mortality for the UK during the 2020s, 2050s and 2080s. *J Epidemiol Community Health, 68*(7), 641-648,
Hauer, M. E. (2019). Population projections for US counties by age, sex, and race controlled to shared socioeconomic pathway. *Scientific data, 6*(1), 1-15,
Heutel, G., Miller, N. H., & Molitor, D. (2021). Adaptation and the mortality effects of temperature across US climate regions. *Review of Economics and Statistics, 103*(4), 740-753,
Hintz, M. J., Luederitz, C., Lang, D. J., & von Wehrden, H. (2018). Facing the heat: A systematic literature review exploring the transferability of solutions to cope with urban heat waves. *Urban Climate, 24*, 714-727,
Jackson, J. E., Yost, M. G., Karr, C., Fitzpatrick, C., Lamb, B. K., Chung, S. H., Chen, J., Avise, J., Rosenblatt, R. A., & Fenske, R. A. (2010). Public health impacts of climate change in Washington State: projected mortality risks due to heat events and air pollution. *Climatic change, 102*(1), 159-186,
Jenkins, K., Hall, J., Glenis, V., Kilsby, C., McCarthy, M., Goodess, C., Smith, D., Malleson, N., & Birkin, M. (2014). Probabilistic spatial risk assessment of heat impacts and adaptations for London. *Climatic change, 124*(1), 105-117,
Kalkstein, L. S., & Greene, J. S. (1997). An evaluation of climate/mortality relationships in

large US cities and the possible impacts of a climate change. *Environmental health perspectives, 105*(1), 84-93,

Knowlton, K., Lynn, B., Goldberg, R. A., Rosenzweig, C., Hogrefe, C., Rosenthal, J. K., & Kinney, P. L. (2007). Projecting heat-related mortality impacts under a changing climate in the New York City region. *American journal of public health, 97*(11), 2028-2034,

Kyselý, J., & Plavcová, E. (2012). Declining impacts of hot spells on mortality in the Czech Republic, 1986–2009: adaptation to climate change? *Climatic change, 113*(2), 437-453,

Lee, J. Y., & Kim, H. (2016). Projection of future temperature-related mortality due to climate and demographic changes. *Environment International, 94*, 489-494,

Li, T., Horton, R. M., Bader, D. A., Zhou, M., Liang, X., Ban, J., Sun, Q., & Kinney, P. L. (2016). Aging will amplify the heat-related mortality risk under a changing climate: projection for the elderly in Beijing, China. *Scientific reports, 6*(1), 1-9,

Lin, Y.-K., Ho, T.-J., & Wang, Y.-C. (2011). Mortality risk associated with temperature and prolonged temperature extremes in elderly populations in Taiwan. *Environmental research, 111*(8), 1156-1163,

Lo, Y. E., Mitchell, D. M., Gasparrini, A., Vicedo-Cabrera, A. M., Ebi, K. L., Frumhoff, P. C., Millar, R. J., Roberts, W., Sera, F., & Sparrow, S. (2019). Increasing mitigation ambition to meet the Paris Agreement's temperature goal avoids substantial heat-related mortality in US cities. *Science advances, 5*(6), eaau4373,

Ma, W., Wang, L., Lin, H., Liu, T., Zhang, Y., Rutherford, S., Luo, Y., Zeng, W., Zhang, Y., & Wang, X. (2015). The temperature–mortality relationship in China: an analysis from 66 Chinese communities. *Environmental research, 137*, 72-77,

Maher, N., Milinski, S., Suarez-Gutierrez, L., Botzet, M., Dobrynin, M., Kornblueh, L., et al. (2019). The Max Planck Institute Grand Ensemble: Enabling the Exploration of Climate System Variability. *Journal of Advances in Modeling Earth Systems, 11*(7), 2050-2069, doi:10.1029/2019ms001639

Marsha, A., Sain, S., Heaton, M., Monaghan, A., & Wilhelmi, O. (2018). Influences of climatic and population changes on heat-related mortality in Houston, Texas, USA. *Climatic change, 146*(3), 471-485,

Martínez-Solanas, È., Quijal-Zamorano, M., Achebak, H., Petrova, D., Robine, J.-M., Herrmann, F. R., Rodó, X., & Ballester, J. (2021). Projections of temperature-attributable mortality in Europe: a time series analysis of 147 contiguous regions in 16 countries. *The Lancet Planetary Health, 5*(7), e446-e454, Mearns, L., McGinnis, S., Korytina, D., Arritt, R., Biner, S., Bukovsky, M., et al. (2017). *The NA-CORDEX dataset, version 1.0. NCAR Climate Data Gateway*.

Muñoz-Sabater, J., Dutra, E., Agustí-Panareda, A., Albergel, C., Arduini, G., Balsamo, G., Boussetta, S., Choulga, M., Harrigan, S., & Hersbach, H. (2021). ERA5-Land: A state-of-the-art global reanalysis dataset for land applications. *Earth System Science Data, 13*(9), 4349-4383,

Muthers, S., Matzarakis, A., & Koch, E. (2010). Climate change and mortality in Vienna—a human biometeorological analysis based on regional climate modeling. *International Journal of Environmental Research and Public Health, 7*(7), 2965-2977,

Petkova, E. P., Vink, J. K., Horton, R. M., Gasparrini, A., Bader, D. A., Francis, J. D., & Kinney, P. L. (2017). Towards more comprehensive projections of urban heat-related mortality: estimates for New York City under multiple population, adaptation, and climate scenarios. *Environmental health perspectives, 125*(1), 47-55,

Samet, J. M., Zeger, S. L., Dominici, F., Curriero, F., Coursac, I., Dockery, D. W., Schwartz, J., & Zanobetti, A. (2000). The national morbidity, mortality, and air pollution study. *Part II: morbidity and mortality from air pollution in the United States Res Rep Health Eff Inst, 94*(pt 2), 5-79,

Takahashi, K., Honda, Y., & Emori, S. (2007). Assessing mortality risk from heat stress due to global warming. *Journal of risk research, 10*(3), 339-354,

Vardoulakis, S., Dear, K., Hajat, S., Heaviside, C., Eggen, B., & McMichael, A. J. (2014). Comparative assessment of the effects of climate change on heat-and cold-related mortality in the United Kingdom and Australia. *Environmental health perspectives, 122*(12), 1285-1292,

Vicedo-Cabrera, A. M., Guo, Y., Sera, F., Huber, V., Schleussner, C.-F., Mitchell, D., Tong, S., Coelho, M. d. S. Z. S., Saldiva, P. H. N., & Lavigne, E. (2018). Temperature-related mortality impacts under and beyond Paris Agreement climate change scenarios. *Climatic change, 150*(3), 391-402,

Wang, Y., Shi, L., Zanobetti, A., & Schwartz, J. D. (2016). Estimating and projecting the effect of cold waves on mortality in 209 US cities. *Environment International, 94*, 141-149,

Weinberger, K. R., Haykin, L., Eliot, M. N., Schwartz, J. D., Gasparrini, A., & Wellenius, G. A. (2017). Projected temperature-related deaths in ten large US metropolitan areas under different climate change scenarios. *Environment International, 107*, 196-204,

Yang, J., Zhou, M., Ren, Z., Li, M., Wang, B., Liu, D. L., Ou, C.-Q., Yin, P., Sun, J., & Tong, S. (2021). Projecting heat-related excess mortality under climate change scenarios in China. *Nature communications, 12*(1), 1-11, Yi, W., & Chan, A. P. (2015). Effects of temperature on mortality in Hong Kong: a time series analysis. *International journal of biometeorology, 59*(7), 927-936,

Zhang, Y., Li, C., Feng, R., Zhu, Y., Wu, K., Tan, X., & Ma, L. (2016). The short-term effect of ambient temperature on mortality in Wuhan, China: a time-series study using a distributed lag non-linear model. *International Journal of Environmental Research and Public Health, 13*(7), 722,